RSC Advances

COMMUNICATION

View Article Online
View Journal | View Issue

Cite this: *RSC Adv.*, 2015, **5**, 11175

Received 15th December 2014
Accepted 7th January 2015

DOI: 10.1039/c4ra16385k

www.rsc.org/advances

Plasmonic-enhanced perovskite solar cells using alloy popcorn nanoparticles†

Zelin Lu,‡[a] Xujie Pan,‡[b] Yingzhuang Ma,[a] Yu Li,[a] Lingling Zheng,[a] Danfei Zhang,[a] Qi Xu,[b] Zhijian Chen,[ac] Shufeng Wang,*[ac] Bo Qu,[ac] Fang Liu,*[b] Yidong Huang,[b] Lixin Xiao*[ac] and Qihuang Gong[a]

This article demonstrates a significant broadband enhancement of light absorption and improvement of photon-generated-charge transfer in $CH_3NH_3PbI_3$ perovskite solar cells by incorporating plasmonic Au–Ag alloy popcorn-shaped nanoparticles (NPs). Compared to conventional nanoparticles and nanorods, these popcorn-shaped NPs have many fine structures. The device's maximum power conversion efficiency (PCE) increases from 8.9% to 10.3%, namely 15.7% enhancement, with the aid of plasmonic popcorn-shaped NPs.

Since the inorganic–organic hybrid perovskite solar cell was first reported in 2009,[1] its power conversion efficiency (PCE) has rapidly improved to as high as 19.3%, and could ultimately boost efficiencies to 25%, as high as that of a single-crystal silicon cell.[2,3] To further improve the efficiency, it is necessary to extend the light absorption spectrum to harvest more energy in thin film solar cells, without increasing the thickness and the complexity of the devices.[4–6] Although the absorption coefficient of hybrid perovskite at 550 nm is around 1.5×10^4 cm^{-1},[7] as strong as organic materials, the absorption is drop-down around the band edge. Therefore, it should be promising to greatly enhance the light absorption of hybrid perovskite around the band edge.

To boost the solar cells' light absorption, one of the promising methods is to apply noble metal nanoparticles, on which localized surface plasmon (LSP) resonance can be excited under the light illumination. The confined electromagnetic energy based on LSP resonance could greatly improve the light absorption of active medium surrounding the nanoparticles (NPs).[8,9] The light absorption enhancement and efficiency improvement of different kinds of solar cells, including thin film Si solar cells, dye-sensitized solar cells (DSSCs),[10–12] and organic photovoltaics (OPVs),[13–16] had been reported recently.

For perovskite solar cells, Snaith *et al.* succeeded in improving cell's efficiency by employing core–shell $Au@SiO_2$ NPs to reduce the exciton binding energy. However, light absorption enhancement had not been observed.[17] The reason might be that the narrow LSP resonant peak resulted from the $Au@SiO_2$ NPs is overlapped with the strong light absorption of perovskite. Since the excitation of LSP mode is closely related to the shapes and components of the metal materials,[18] irregular alloy NPs with many fine structures are conducive to support panchromatic LSP resonance and broadband optical absorption enhancement.[19]

In this article, we introduced the irregular Au–Ag alloy "popcorn-shaped" NPs (hereafter referred to as "popcorn NPs") into perovskite solar cells. Different from the results of $Au@SiO_2$ NPs,[17] these plasmonic popcorn NPs exhibited broadband LSP resonances from ultraviolet to near-infrared wavelength range. With the aid of the popcorn NPs, the optical absorption property of the perovskite layer was improved significantly, especially at the long wavelength region near band edge, which is indicated by the optical absorption spectra and incident photon-to-current efficiency (IPCE). Moreover, the electron transfer property of the device was also improved, which is different from our previously reported results in DSSCs.[19] These results suggest a valuable way to simultaneously improve the broadband light absorption and the charge transfer properties, which can be expected to further increase the efficiency of various perovskite solar cells, including unleaded perovskite cells suffering from low efficiencies and even the leaded perovskite cells with rather high efficiencies.

The transmission electron microscopy (TEM) image of a popcorn NP is shown in Fig. 1a, which presents many fine structures of different shape, with an average size of 150 ± 50

[a]*State Key Laboratory for Mesoscopic Physics and Department of Physics, Peking University, Beijing 100871, China. E-mail: wangsf@pku.edu.cn; xiao66@pku.edu.cn*

[b]*Department of Electronic Engineering, Tsinghua National Laboratory for Information Science and Technology, Tsinghua University, Beijing 100084, China. E-mail: liu_fang@tsinghua.edu.cn*

[c]*New Display Device and System Integration Collaborative Innovation Center of the West Coast of the Taiwan Strait, Fuzhou 350002, China*

† Electronic supplementary information (ESI) available: Energy dispersive spectroscopy spectra, method details and optical absorption of thin perovskite films. See DOI: 10.1039/c4ra16385k

‡ These authors contribute equally to this paper.

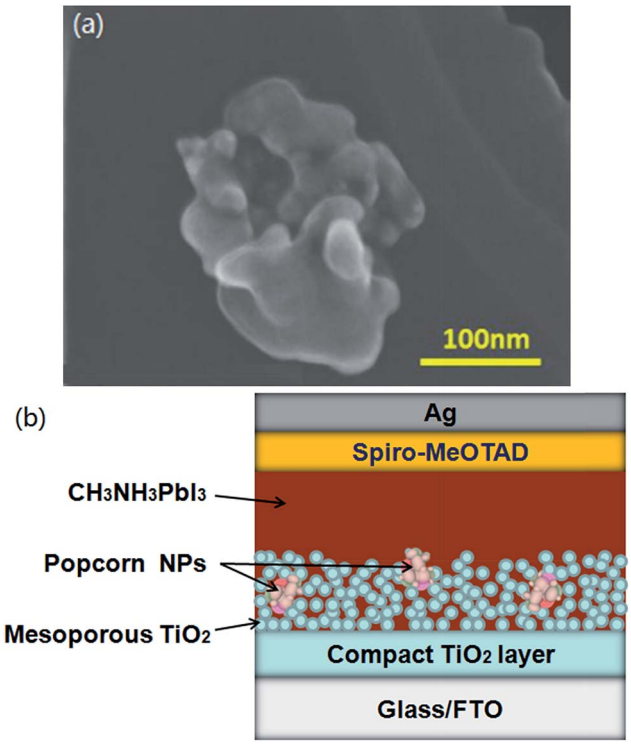

Fig. 1 (a) TEM image of a popcorn NP. (b) Illustrative structure of the perovskite solar cell with popcorn NPs embedded in the mesoporous TiO_2 framework.

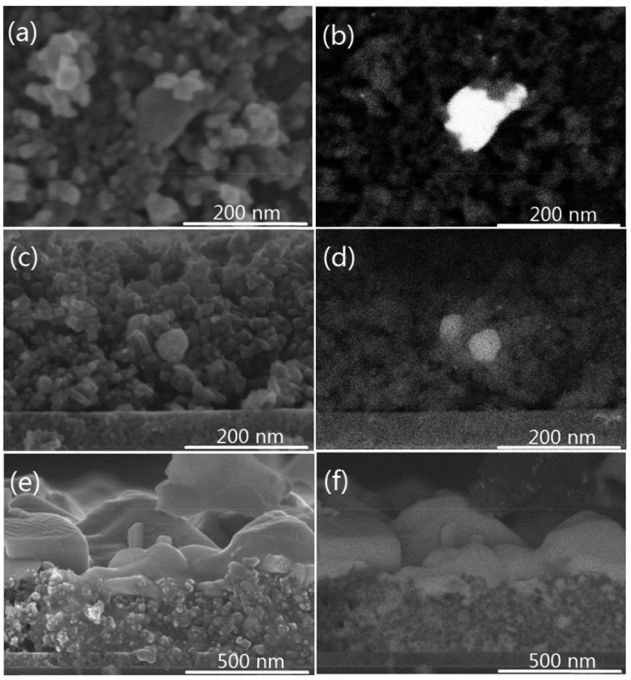

Fig. 2 SEM images of popcorn NPs within mesoporous TiO_2 framework: (a) top view, secondary electron image; (b) top view, backscattered electron image; (c) cross-section view, secondary electron image; (d) cross-section view, backscattered electron image. SEM images of perovskite on mesoporous TiO_2: (e) secondary electron image; (f) backscattered electron image.

nm. The unique popcorn NPs have the advantage of exciting various LSP modes in a wide solar spectrum range.[19] Therefore, a broad wavelength range of optical absorption and improvement of device performances are expected with the aid of these popcorn NPs. The schematic structure of the device is shown in Fig. 1b. To avoid compromising the morphology of the perovskite layer, the popcorn NPs were embedded into the TiO_2 mesoporous framework.

In order to identify popcorn NPs in the mesoporous TiO_2 framework, scanning electron microscopy (SEM) images are taken and shown in Fig. 2. From the secondary electron image of the top view in Fig. 2a, a gray popcorn NP is partially exposed at the surface of the film, which is more visible in the corresponding backscattered electron image (Fig. 2b). From the secondary electron image of the cross-section view in Fig. 2c, a popcorn NP is found embedded in the mesoporous TiO_2 layer, which can be more distinguishable in the backscattered electron image due to stronger contrast (Fig. 2d). This is further confirmed by the corresponding energy dispersive spectroscopy (see ESI Fig. S1†). After preparing a perovskite photoactive layer on the mesoporous TiO_2 (Fig. 2e and f), the perovskite fills into the pores of the mesoporous TiO_2 layer and forms a cover layer, and no significantly influence could be observed on the perovskite crystalline formation in the presence of popcorn NPs.

When these NPs were blended into the mesoporous TiO_2 framework, slight increase in optical absorption was found as shown in Fig. 3a. After filling perovskite into the mesoporous framework, the device's optical absorption was strikingly enhanced, especially at long wavelength range starting from 580 nm to near-infrared due to light trapping of LSP resonance (Fig. 3b). From the transmittance spectra, we can infer that light absorption is saturated in the short wavelength range ($\lambda_0 < 580$ nm). That is why no prominent light harvesting enhancement is presented from 300 to 580 nm in the absorption spectra. With this fact in mind, we fabricated thinner perovskite films to further investigate the NPs' plasmonic effect on light absorption. It turned out that broadband (from 370 to 800 nm) light absorption is achieved by popcorn NPs in thinner perovskite films (see ESI Fig. S2†). At short wavelength range where light absorption is not saturated in these thinner films, distinctly optical absorbance enhancement can also be observed. This result confirms the broadband plasmonic effects of the popcorn NPs, and their effectiveness of promoting light harvesting in perovskite-based solar cells.

To investigate the effectiveness of NPs, perovskite solar cells with and without NPs were fabricated. Fig. 4a shows the photovoltaic performance of two kinds of devices. It is clearly demonstrated that both V_{oc}, J_{sc} are increased after popcorn NPs were incorporated into the devices, thereby leading to an increase in PCE. Compared with 8.9% for the maximum PCE of the devices without NPs, the maximum PCE of the ones with NPs reaches 10.3%, which accounts for an about 15.7% enhancement measured under AM 1.5G (100 mW cm^{-2}), as list in Table 1. The current density to voltage characteristics (J–V curves) of the best-performance device are shown in Fig. 4b. The

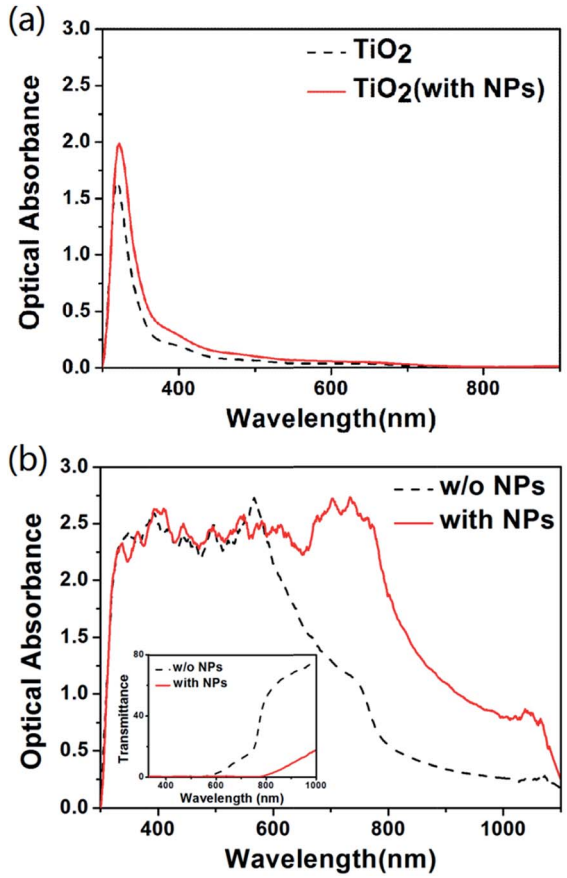

Fig. 3 (a) Optical absorption spectra of mesoporous TiO_2 layer with and without popcorn NPs. (b) Optical absorption of perovskite film on mesoporous TiO_2 framework with and without popcorn NPs. The inset shows the transmittance spectra.

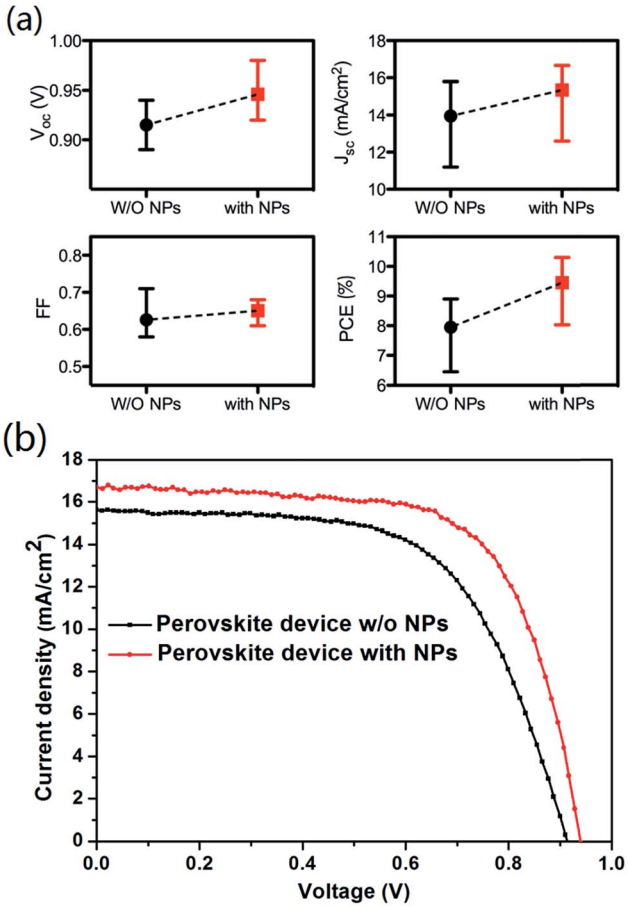

Fig. 4 (a) The photovoltaic performance of 25 individual devices (red: devices with popcorn NPs; black: control devices). (b) *J*–*V* curves of the best-performance perovskite device with and without popcorn NPs, respectively.

J_{sc} shows an obvious increase which is resulted from the LSP-enhanced optical absorption. The enhancement of V_{oc} can be due to the suppression of charge recombination in the presence of NPs, which will be discussed later.

Fig. 5a shows the IPCE spectra of the devices. The IPCE of the device with NPs shows a steady increment compared with the one without NPs over the entire wavelength range. Fig. 5b shows the enhancement ratio of IPCE of the two devices, providing an intuitive view of the IPCE enhancement. It is obvious that, around the band edge, the IPCE of plasmonic device sharply increases. According to the integral of IPCE weighted by the solar spectrum, the predicted J_{sc} value could be estimated. For the NPs-free case, the integration value of J_{sc} is 14.31 mA cm^{-2}, and for the NPs-incorporated case, the value increases to 16.21 mA cm^{-2}, consistent well with the actually measured J_{sc} values of 14.9 mA cm^{-2} and 16.43 mA cm^{-2}, respectively.

According to the results shown in Fig. 5, three facts should be noticed here. Firstly, throughout the spectra shorter than 720 nm, the broadband enhancement clearly contributes to the final output. Secondly, in the wavelength range shorter than 580 nm, where the absorption is saturated even without NPs and thus almost no absorption enhancement could be observed as shown in Fig. 3b, but the IPCE is still enhanced. This interesting result indicates that the cell's efficiency improvement does not only depend on the light absorption enhancement but also other factors. As we will discuss later, this increment of IPCE might be due to charge transporting behavior improvement with the presence of NPs. Thirdly, the IPCE enhancement around band edge between 720–820 nm is very sensitive to the amount of light absorbed, the aid of NPs is very effective to increase IPCE in this range. These results suggest a valuable way to simultaneously improve broadband light absorption and charge transfer properties for perovskite solar cells.

Table 1 The best performance of perovskite cells with and without NPs

Device	V_{oc} (V)	J_{sc} (mA cm^{-2})	FF	PCE (%)
w/o NPs	0.92	15.51	0.63	8.9
With NPs	0.95	16.46	0.66	10.3

To understand the functions of the popcorn NPs on charge transfer, we measured the charge generation and transfer properties in the perovskite photovoltaic cells *via* steady-state

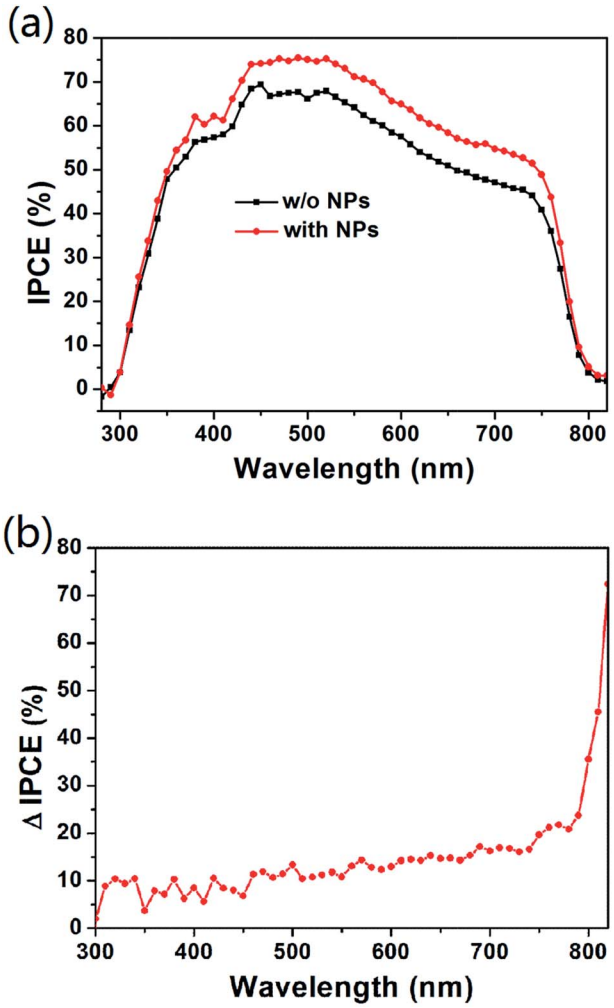

Fig. 5 (a) IPCE spectra (from 280 nm to 820 nm) of devices with and without Au–Ag alloy popcorn NPs. (b) IPCE enhancement ratio (ΔIPCE) of the perovskite devices. $\Delta IPCE = (IPCE_{with\ NPs}(\lambda) - IPCE_{w/o\ NPs}(\lambda))/IPCE_{w/o\ NPs}(\lambda) \times 100\%$, where $IPCE_{with\ NPs}(\lambda)$ and $IPCE_{w/o\ NPs}(\lambda)$ are the IPCEs of the perovskite devices with and without popcorn NPs at wavelength of λ, respectively.

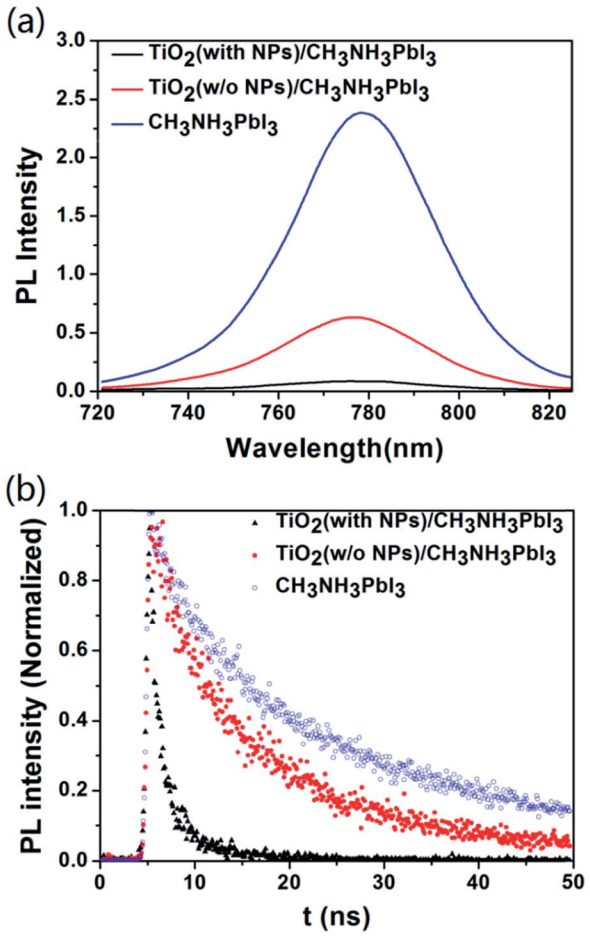

Fig. 6 Steady-state (a) and time-resolved (b) PL of $CH_3NH_3PbI_3$, TiO_2/$CH_3NH_3PbI_3$, and TiO_2 (with popcorn NPs)/$CH_3NH_3PbI_3$ films.

photoluminescence (PL) and time-resolved photoluminescence characterization. The steady-state PL of $CH_3NH_3PbI_3$, TiO_2/$CH_3NH_3PbI_3$, and TiO_2 (with NPs)/$CH_3NH_3PbI_3$ films are presented in Fig. 6a. A significant quenching effect (reduced to ~30%) can be observed when the mesoporous TiO_2 forms a contact with $CH_3NH_3PbI_3$. Almost completely PL quenching is shown when popcorn NPs are embedded into the TiO_2 mesoporous framework, indicating efficient charge separation at the TiO_2/perovskite interface. This reinforced behavior is caused by the strengthened localized electric field of LSP around the metallic NPs.[20,21]

So as to further confirm these charge transfer processes, the time-resolved photoluminescence was measured as shown in Fig. 6b. The lifetime of the carriers in devices can be obtained by fitting the data as reports.[17,22] For the perovskite neat film, a PL lifetime of 10.2 ns is obtained, which is consistent with the previous report.[23] When the perovskite is filled into the mesoporous TiO_2, the PL lifetime reduces to 7.8 ns. Surprisingly, for the TiO_2/NPs case, the carrier lifetime further drops to 0.99 ns. Considering the improved PCE of cells, the faster charge transfer from perovskite to TiO_2/NPs than to TiO_2-only film could be one of the reasons for strikingly dropped lifetime. Namely, the strong PL quenching might be caused by the LSP-induced faster charge transfer at the interface, resulting in the suppression of charge recombination, therefore V_{oc} should be increased as mentioned above.

Conclusions

In summary, the light absorption enhancement and electron transfer improvement in perovskite solar cells have been achieved by incorporating plasmonic Au–Ag alloy popcorn-shaped NPs. Owing to the alloy components and fine structures of popcorn NPs, the broadband optical absorption enhancement in perovskite solar cells has been obtained, especially around the band edge between 720–820 nm, where the IPCE enhancement is sharply. Moreover, the steady-state and transient PL studies also indicate that plasmonic popcorn NPs can lead to faster charge transfer at the TiO_2/perovskite interface, resulting in PCE enhancement. Based on the two beneficial functions of

popcorn NPs, the maximum PCE of perovskite solar cells has been enhanced by 15.7%, from 8.9% to 10.3%. With the merit of simultaneously improving the light absorption and the charge transfer properties, it is expected to apply the plasmonic popcorn NPs for further increasing the PCE of solar cells, such as unleaded cells currently with low efficiency, and the leaded cells already have top efficiency.

Acknowledgements

This study was financially supported by the National Natural Science Foundation of China (61177020, 11121091, 61107050) and the National Basic Research Program of China (2013CB328704, 2013CBA01704).

References

1 A. Kojima, K. Teshima, Y. Shirai and T. Miyasaka, *J. Am. Chem. Soc.*, 2009, **131**, 6050–6051.
2 R. F. Service, *Science*, 2014, **344**, 458.
3 H. Zhou, Q. Chen, G. Li, S. Luo, T.-B. Song, H.-S. Duan, Z. Hong, J. You, Y. Liu and Y. Yang, *Science*, 2014, **345**, 542–546.
4 Y. Ogomi, A. Morita, S. Tsukamoto, T. Saitho, N. Fujikawa, Q. Shen, T. Toyoda, K. Yoshino, S. S. Pandy, T. Ma and S. Hayase, *J. Phys. Chem. Lett.*, 2014, **5**, 1004–1011.
5 F. Hao, C. C. Stoumpos, D. H. Cao, R. P. H. Chang and M. G. Kanatzidis, *Nat. Photonics*, 2014, **8**, 489–494.
6 N. K. Noel, S. D. Stranks, A. Abate, C. Wehrenfennig, S. Guarnera, A. A. Haghighirad, A. Sadhanala, G. E. Eperon, M. B. Johnston, A. M. Petrozza, L. M. Herz and H. J. Snaith, *Energy Environ. Sci.*, 2014, **7**, 3061.
7 S. Kazim, M. K. Nazeeruddin, M. Grätzel and S. Ahmad, *Angew. Chem., Int. Ed.*, 2014, **53**, 2812–2824.
8 X. Huang, S. Neretina and M. A. El-Sayed, *Adv. Mater.*, 2009, **21**, 4880–4910.
9 H. Chen, L. Shao, Q. Li and J. Wang, *Chem. Soc. Rev.*, 2013, **42**, 2679–2724.
10 S. D. Standridge, G. C. Schatz and J. T. Hupp, *J. Am. Chem. Soc.*, 2009, **131**, 8407–8409.
11 M. D. Brown, T. Suteewong, R. S. Kumar, V. D'Innocenzo, A. Petrozza, M. M. Lee, U. Wiesner and H. J. Snaith, *Nano Lett.*, 2011, **11**, 438–445.
12 J. Qi, X. Dang, P. T. Hammond and A. M. Belcher, *ACS Nano*, 2011, **5**, 7108–7116.
13 D. H. Wang, K. H. Park, J. H. Seo, J. Seifter, J. H. Jeon, J. K. Kim, J. H. Park, O. O. Park and A. J. Heeger, *Adv. Energy Mater.*, 2011, **1**, 766–770.
14 S. W. Baek, J. Noh, C. Lee, B. S. Kim, M. K. Seo and J. Y. Lee, *Sci. Rep.*, 2013, **3**, 1726–1732.
15 L. Lu, Z. Luo, X. Tao and L. P. Yu, *Nano Lett.*, 2013, **13**, 59–64.
16 X. Li, W. C. H. Choy, L. Huo, F. Xie, W. E. I. Sha, B. Ding, X. Guo, Y. Li, J. Hou, J. You and Y. Yang, *Adv. Mater.*, 2012, **24**, 3046–3052.
17 W. Zhang, M. Saliba, S. D. Stranks, Y. Sun, X. Shi, U. Wiesner and H. J. Snaith, *Nano Lett.*, 2013, **13**, 4505–4510.
18 A. V. Zayats, I. I. Smolyaninov and A. A. Maradudin, *Phys. Rep.*, 2005, **408**, 131–314.
19 Q. Xu, F. Liu, Y. Liu, K. Cui, X. Feng, W. Zhang and Y. Huang, *Sci. Rep.*, 2013, **3**, 2112–2118.
20 Q. C. Sun, H. Mundoor, J. C. Ribot, V. Singh, I. I. Smalyukh and P. Nagpal, *Nano Lett.*, 2014, **14**, 101–106.
21 J. N. Li, T. Z. Liu, H. R. Zheng, F. Gao, J. Dong, Z. L. Zhang and Z. Y. Zhang, *Opt. Express*, 2013, **21**, 17176–17185.
22 J. You, Z. Hong, Y. Yang, Q. Chen, M. Cai, T. B. Song, C. C. Chen, S. Lu, Y. Liu, H. Zhou and Y. Yang, *ACS Nano*, 2014, **8**, 1674–1680.
23 S. D. Stranks, G. E. Eperon, G. Grancini, C. Menelaou, M. J. P. Alocer, T. Leijtens, L. M. Herz, A. Petrozza and H. J. Snaith, *Science*, 2013, **342**, 341–345.